

Simulation and Verification of Lake Ontario's Mean State¹

JOSEPH CHI KAN HUANG² AND PETER W. SLOSS³

Great Lakes Environmental Research Laboratory, NOAA, Ann Arbor, MI 48104

(Manuscript received 1 August 1980, in final form 21 August 1981)

ABSTRACT

A numerical dynamic model based on primitive equations has been developed for Lake Ontario. Many experimental tests for parameter selections and alternative formulations of physical processes in the model were carried out. Two simulations, both repeated in July and December 1972, one under constant atmospheric forcing and the other under hourly time-dependent, spatially varying atmospheric forcing, are presented here. With constant southwesterly wind parallel to the major axis of the lake, as was the case in both July and December 1972, the steady-state lake circulation forms a typical two-gyre wind-driven pattern with currents flowing with the wind in both coastal regions and return flow in the middle of the lake. The monthly mean currents of the hourly time-dependent variable-forcing simulation of December have a pattern similar to that of the constant-forcing case, while the mean currents of the July time-dependent variable-forcing simulation yield a single cyclonic circulation pattern with currents flowing against the mean wind in the north shore, which is totally different from the constant-forcing steady-state result. Both the monthly mean model currents of the time-dependent variable-forcing simulations agree very well with the monthly mean currents observed over Lake Ontario during the International Field Year for the Great Lakes (IFYGL).

When the lake density is nearly homogeneous, with negligible thermal effects, as in December, the lake response is mostly barotropic. The induced circulation consists of dominantly wind-driven currents adjusted to the bottom topography with a thin Ekman layer on top of the geostrophically balanced currents in deep layers. Further simplification of the dynamics is a consequence of the linear nature of the model's behavior. The means of the time-dependent variable-forcing simulation merge to form the constant-forcing steady-state circulation. In July, however, the lake is stratified and both the wind-driven and thermal-driven currents are important. It seems that the final circulation pattern in a lake depends mostly on the relative strengths of the thermally affected mechanisms and the wind-driven mechanism. Dominance of the former generally results in a one-gyre circulation pattern, while dominance of the latter results in a two-gyre circulation pattern. In a constant-forcing model, most of the thermally affected mechanisms, such as the rectified effect, the coastal mixing, dome-shaped isotherms, and horizontal and vertical density gradients, are obscured by the fully developed wind-driven steady-state currents. Employing such a model to simulate the stratified lake is definitely inadequate and misleading because only the time-dependent variable-forcing simulation results in a mean, single-gyre circulation pattern that matches the observations, while the constant-forcing still produces an unrealistic two-gyre circulation pattern for July 1972 (during IFYGL).

1. Introduction

One of the major difficulties in numerical simulation studies for oceans and large lakes is the lack of reliable observational data (both in atmospheric forcing and in oceanic or lake responses) for proper verifications of the model. This is particularly true for the low-frequency fluctuations in an ocean or lake. For example, the North Pacific Ocean is considered the most frequently surveyed ocean, but with all the historical oceanographic data accumu-

lated, there are still many areas as large as 5° longitude × 5° latitude without a single reliable measurement. In the Great Lakes, the situation is not much better and, consequently, numerical studies have been restricted to certain observable phenomena, such as seiches and storm surges. However, after the April 1972–March 1973 International Field Year for the Great Lakes (IFYGL), Lake Ontario became the best surveyed large body of water suitable for simulation studies because of the systematically observed and analyzed data available for validation of hydrodynamic models. One of the major objectives of the IFYGL program was to document the long-term mean temperature and current patterns in Lake Ontario. Much attention has been focused on the monthly mean state of the lake in the course of post-IFYGL data analyses mostly because monthly

¹ GLERL Contribution No. 227.

² Present affiliation: Office of Research and Development, NOAA, Rockville, MD 20852.

³ Present affiliation: National Geophysical and Solar-Terrestrial Data Center, Environmental Data Information Service, NOAA, Boulder, CO 80303.

means are averaged over a time period that is long enough to smooth out transient phenomena without much effect of seasonal variabilities. At present, the first-order descriptions of the monthly mean circulation and density structure in Lake Ontario are available.

Numerical studies for Lake Ontario were carried out by Simons (1974) in conjunction with the IFYGL field programs. Simons' model took most physical processes into consideration, including the free surface dynamics, and has been verified extensively with IFYGL current and water level data, mostly on episodic responses (Simons, 1974, 1975, 1976). However, Simons did not attempt to verify his model with mean circulation patterns in the lake. Since then, more data have been processed and accumulated in the IFYGL data bank. Bennett (1977) developed a similar model with a rigid-lid approximation. As Bennett pointed out, his uniform coarse grid models fail to reproduce certain observational results, such as the against-wind flow and the large depression of the thermocline along the north shore. The simulated flow on the north shore and the Kelvin wave episodes were improved by a much finer resolution along the coastal zone (Bennett, 1977). In verifications, Bennett (1977, 1978) relied heavily on the nearshore, coastal-chain data during IFYGL. As pointed out by Csanady and Scott (1980), the coastal chain data were subject to fair weather bias, which definitely resulted in a much more stable and homogeneous air condition near the air-water interactive layer. This might be the reason Bennett (1977) took a simple constant coefficient stress law that eliminates one of the important mechanisms in generating the cyclonic circulation pattern in lakes, as we will point out in the next section. Furthermore, the stretched coordinate technique, first used by Bryan and Cox (1967) near the western boundary in the ocean, is not practical for a simulation domain of irregular boundaries because Bennett had to sacrifice the real configuration of the lake for a rectangular shape.

In an effort to verify the monthly mean state in the lake, a time-dependent three-dimensional numerical model for Lake Ontario containing grid representations of the actual coastal configuration and bottom topography of the lake has been developed to simulate the organized water motions and thermal structure in the lake and to aid in understanding the physical nature of the lake in response to atmospheric forcing. The model is based on primitive equations in which the mean motions and temperature field in the lake are produced by surface wind stress and atmospheric heating. The simulation model we employed is not unlike those of Simons (1974) and of Bennett (1977); however, the boundary-layer atmosphere-lake interactions are treated in a different manner. We try to show that, if the atmos-

pheric stability is taken into account in the air-water coupled interactions and reliable atmospheric data are available, a reasonably coarse, uniform grid model is capable of reproducing a realistic mean circulation pattern and thermal structure in the lake. We will also show that based on dynamic analysis, the mean circulation pattern of a homogeneous lake under time-dependent, variable atmospheric forcing will merge into a similar wind-driven circulation pattern under constant atmospheric forcing since the lake is dominantly influenced by the mechanical stress input. In a stratified lake, the thermally affected mechanisms are as important as the wind stresses, and the time-dependent, variable atmospheric forcing results in a more realistic simulation when compared to observations, while the simulation of the constant atmospheric forcing yields an unrealistic circulation pattern. This paper briefly describes the numerical model, summarizes major current-generating mechanisms in a homogeneous and in a stratified lake, and shows analyses and comparisons with observations of two December and two July simulations, one each under steady, constant atmospheric forcing and the others under time-dependent, variable atmospheric forcing. The winter simulation shows that when the lake is homogeneous and the wind is moderately strong, as in the December case, the lake circulation forms a two-gyre pattern and the mean time-dependent variable-forcing currents merge to a pattern similar to that produced by the constant forcing. For simulation of a summer stratified lake, where the importance of the boundary-layer formulation and the thermally affected mechanisms are intensified, the constant atmospheric forcing still reveals a two-gyre pattern similar to that of winter, but the mean time-dependent variable-forcing currents form a lake-wide, one-gyre cyclonic circulation pattern with flow against the mean wind along the north shore—a pattern totally different from that of the constant-forcing steady-state results. One dynamic explanation is that in a stratified lake, with the exception of direct wind forcing, all thermally affected mechanisms, such as the internal pressure adjustment induced by the dome-shaped isotherms, the differential bottom friction due to the unevenness in stratifications, and the local surface stress curl caused by the surface temperature gradients, are competing with the mean wind effect and thus result in the observed mean cyclonic pattern. In the July case, all currents generated by thermally affected mechanisms possess strong cyclonic vorticity. It seems that the final circulation pattern in a lake depends mostly on the relative strength of the combined effect of these thermally affected mechanisms as compared with the effect of the direct wind-driven currents that interact with the lake topography and generally result in a two-gyre circulation

pattern. If the thermal effect is dominant, it, together with the lake-scale wind-curl effect, forms a one-gyre circulation pattern. The dynamic mechanisms probably responsible for producing the mean lake state and a brief description of the model, together with the atmosphere-lake boundary interactions, are presented in Section 2; simulation results in Section 3, comparisons and discussions in Section 4; and conclusions and critiques in the last section. We should point out that in this study detailed model comparisons are not attempted. We simply present our simulation results, explain how they were obtained, and offer our interpretations.

2. Theoretical considerations and the dynamic model

In studying the dynamics of lake circulation, these are essentially two major energy inputs to the lake, the momentum flux and heat flux through atmospheric forcing, which drive the circulation and determine the density distribution. During the lake warming-up season, thermally induced currents produced through differential heating are dominant and, as a result, a lake-wide cyclonic circulation pattern prevails (Huang, 1971; Csanady, 1977). The interesting phenomenon of a thermal bar appears in late spring or early summer (Huang, 1972). Wind-driven circulation is dominant when the lake is nearly homogeneous. A typical response of a homogeneous lake is that, as the wind blows, the Ekman dynamics dominate the surface flow and result in currents drifting to the right of the wind in the open lake. In the shallow regions, currents are with the wind. An against-the-wind pressure gradient is developed, mostly because of the wind setup; thus return flow forms in the middle of the lake as well as in the deep water. The wind-induced bottom slope current and the principle of conservation of potential vorticity in the presence of irregular bottom topography dominate the barotropic mode (Saylor *et al.*, 1981). When the lake becomes either horizontally or vertically stratified, the thermally induced baroclinic currents are as important as the wind-driven currents. For the sake of understanding the general lake circulation, in regard to the cyclonic pattern in particular, various dynamic mechanisms have been proposed and some of these seem to relate convincingly to observations. Emery and Csanady (1973) suggested that the different wind drags over the colder upwelled and the warmer downwelled water introduce a cyclonic surface stress curl over the lake, and hence cause the cyclonic circulation in the lake. Wunsch (1973) showed that the Lagrange drift induced at second order by internal Kelvin waves has a cyclonic component near the surface. Bennett (1975) offered another explanation: The effect of uneven stratification results in a stronger current at the down-

welling shore, which leads to the resultant cyclonic circulation. Csanady (1975) indicated that the cross-wind nonlinear momentum flux in the Ekman layer fortifies the coastal jet to the right of the wind and reduces the strength of the left one, yielding a cyclonic mean circulation. Csanady (1977) later suggested that during the heating season the combination of surface wind drift and solar heating causes the horizontal transport of some of the absorbed heat into the coastal regions. Bennett (1978) attributes the coastal warming to the rectified effects of the wind-driven upwellings and downwellings of the thermocline. Consequently, the mean isotherm surfaces are domed in shape and the cyclonic, geostrophic mean circulation is generated by the internal pressure distribution. In the model formulation at least all these major mechanisms, together with the proper treatment of the bottom topography, should be taken into consideration.

The model we developed, which is based on primitive equations with the Boussinesq, the hydrostatic and the rigid-lid approximations, contains gridded representations of the actual coastal configurations and bottom topography of Lake Ontario as shown in Fig. 1a. All major physical processes and dynamic mechanisms are taken into account, including nonlinear effects and diffusive effects. The space-staggered grid and the energy conserving, finite-difference scheme are similar to those adopted in ocean models (e.g., Huang, 1973; Haney, 1974). The grid system of the simulation model and the IFYGL current-meter mooring stations are shown in Fig. 1b. The major improvement in this model, as compared with other numerical lake models, is the treatment of the upper boundary conditions. The upper boundary condition is specified in such a manner that boundary-layer dynamics are coupled to the observed atmospheric parameters, thus imposing closer-to-realistic atmosphere-lake interactions. The downward heat flux into the lake is determined by the balance in the atmospheric heat budget equation in the boundary layer. The effects of atmospheric stability near the air-water interface on the momentum and heat flux into the lake are also taken into consideration. Since this part of boundary parameterizations leads to one of the important cyclonic current generation mechanisms, namely, the Emery-Csanady (1973) mechanism, we will show the formulation of surface stress, which depends on the stability of the air-lake interactive layer.

Momentum flux at the lake-atmosphere interface is expressed as a function of the surface wind (V_a) proportional to the momentum exchange coefficient C_D as

$$\pi = \rho_a C_D |V_a| V_a, \quad (1)$$

where ρ_a is the air density, V_a the wind vector and π the surface stress vector.

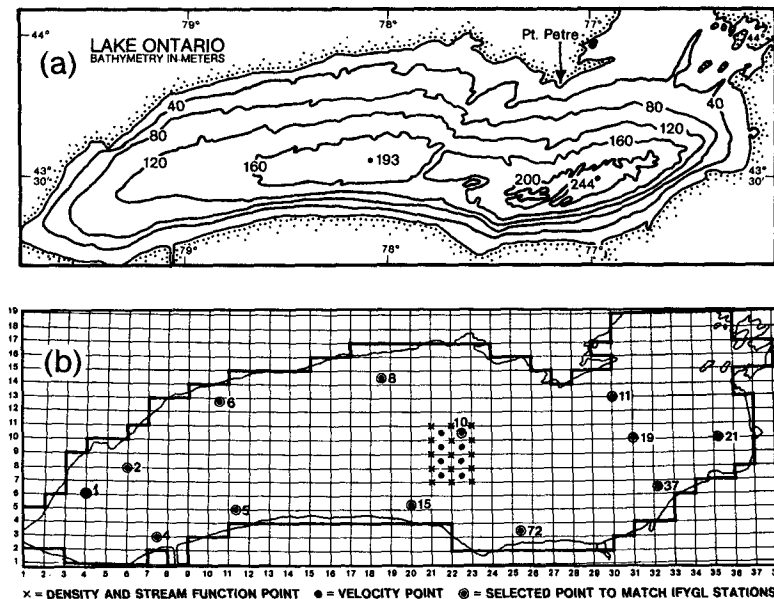


FIG. 1. Lake Ontario with bathymetry (a) and grid system of the simulation model together with IFYGL mooring stations (b).

Because of the persistent surface water temperature differences between the north and the south, and between the east and the west in the lake (e.g., see Fig. 11), the effects of atmospheric stability near the air-water interface on the momentum and heat transfer into the lake should be taken into account. Following Deardorff (1968), the drag coefficient of momentum is a function of the atmospheric stability as

$$C_D = (C_D)_N \exp(-2\beta_v Ri) \quad \text{for stable cases } (Ri > 0), \quad (2a)$$

$$C_D = (C_D)_N \left[1 + \frac{7}{b_1} \ln(1 - b_1 Ri) \right] \quad \text{for unstable cases } (Ri < 0), \quad (2b)$$

where Ri is the bulk Richardson number, a parameter used to measure the stability of the atmosphere,

$$Ri = \frac{gz_{10}}{T_{v0} V_a^2} \left[(T_a - T_s) + 0.38 T_a \frac{(e_a - e_s)}{P_a} \right], \quad (3)$$

wherein T is the temperature, e the vapor pressure and β_v , $(C_D)_N$, b_1 , Z_{10} , and T_{v0} , constants adopted from observations (Businger *et al.*, 1971) as listed in Table 1. Details of the finite-difference equations and the computational schemes, together with the proper treatments of boundary conditions and bathymetry, can be found in Huang (1977, 1978). Note that the empirical constants in Table 1, adopted from maritime meteorological data, have not been systematically verified with lake atmospheric data. Our calculations indicate that values of exchange

coefficients computed by using Table 1 are slightly lower than the values generally used.

3. Model results

Simulations were carried out with space separations of ~5 km in the offshore direction and 8 km in the longshore direction, and with seven variable thickness layers of 10, 10, 20, 20, 30, 50 and 60 m in the vertical. The layer depths are designed to match the maximum number of current meters used during IFYGL. The actual depth of the water column at a grid point is taken into account by adjust-

TABLE 1. Empirical constants in air-water interactions.

Parameter of constant	Symbol	Value	Unit
Air density	P_a	1.23×10^{-3}	$g \text{ cm}^{-3}$
Drag coefficient under neutral state	$(C_D)_N$	2.5×10^{-3}	nondimensional
Constants in drag coefficients	b_1	52.9	nondimensional
Constant in Richardson number	β_v	4.7	nondimensional
Reference height in Richardson number	Z_{10}	10^8	cm
Reference temperature in Richardson number	T_{v0}	290	K

ing the thickness of the deepest layer to make the accumulated thicknesses equal to the actual depth at the point. Since the model conserves mass and energy through the use of a simplified version of the Arakawa (1966) scheme and the rigid-lid approximation is used, a time step of 1.2 h (1.0 h for the time-dependent runs to match input data), based on the Courant-Fredericks-Lewy condition, is used throughout this study. Values for the horizontal and vertical viscosities are $10^6 \text{ cm}^2 \text{ s}^{-1}$ and $25 \text{ cm}^2 \text{ s}^{-1}$ ($50 \text{ cm}^2 \text{ s}^{-1}$ for time-dependent runs), respectively. The values of the diffusivities used are about one order of magnitude smaller. A bottom drag coefficient of 0.0025 for bottom stress is used. Note that after many test runs and analyses, we have bypassed the computation of the nonlinear terms in the momentum equations because of their minor contributions in the present coarse-grid version of the model, a conclusion similar to that arrived at by Simons (1974) and Bennett (1977). However, in the energy equation, the nonlinear rectified effect of the wind-driven upwellings and downwellings of the thermal field (Bennett, 1978) is retained. As will be shown later, this effect is important in the resulting cyclonic circulation pattern in summer.

a. Winter simulations

Three separate December simulations were performed to examine the typical winter state circulations in the lake. The first experiment was run under the December mean atmospheric forcing. The surface wind and air temperature, together with other meteorological parameters for computing heat flux, were obtained from IFYGL monthly lakewide mean data. The lake temperature distribution was set to a quasi-homogeneous state equivalent to the mean state for the end of November, but with no motion as the initial condition of the lake. This experiment was run for 30 days under constant atmospheric forcing; the second experiment under daily variable atmospheric forcing, and the third experiment under the hourly variable atmospheric forcing. Both have spatial variations; the same initial conditions were used.

1) CONSTANT FORCING

The resultant southwesterly wind of December 1972 was nearly parallel to the longshore axis of the lake (Pickett, 1977). The monthly mean surface wind speed is 4.5 m s^{-1} . The net heat flux in December is from the lake to the atmosphere at a rate of $\sim 294 \text{ cal cm}^{-2} \text{ day}^{-1}$ (Pinsak and Rodgers, 1978). Starting from the state of no motion, the dominant features in the lake in the spin-up stage are the inertial oscillations at periods near 17.6 h. Forced inertial motions are generally 180° out of phase between the

upper and lower layers, as commonly observed (Simons, 1974), and result in strong shear currents. As monitoring indicators for the model evolution and numerical stability, all components of kinetic and potential energy are computed and plotted at every time step. According to energy variations, an equilibrium state is reached over 30 days under constant forcing.

Fig. 2a shows the transport streamfunction after 30-days integration under the constant atmospheric forcing of December. Mostly under the influence of the wind, the mass transport function forms a two-gyre circulation pattern, an elongated, anticyclonic gyre dominantly in the north and a cyclonic gyre in the south with a nodal line roughly parallel to the contour of the maximum bottom depth in the southern lake. The anticyclonic gyre is about three times as intense as the cyclonic one. The transport streamfunction pattern indicates that the flow is mostly eastward (with the wind) in the shallow regions and westward (against the wind) in the middle and deep layer of the lake. It shows the typical dynamic response of a lake under the wind-dominated conditions, and the return flow in the middle and deep layer of the lake is caused mostly by the pressure gradient due to wind setups. A similar flow pattern has been modeled from similar wind conditions in Lake Ontario by others, notably Rao and Murty (1970) and Simons (1974).

Fig. 3 contains the current vector plots of the surface layer (Fig. 3a), of the 15 m depth layer (Fig. 3b), and of the 75 m depth layer (Fig. 3c) to match the depths of current meters. Fig. 3a shows that surface currents in both the northern and southern coastal shallow waters generally flow with the wind and that surface currents in the open lake away from the boundaries shift to the right following Ekman dynamics. The coastal jets are clearly developed. Maximum currents reach 16 cm s^{-1} along the northern coast and 12 cm s^{-1} along the southern coast. Upwellings due to the divergent flow in the boundary layer are shown along the northern coast and downwellings are shown along the southern coast. In the deep layers, weak return flows against the surface wind are dominant.

2) TIME-DEPENDENT VARIABLE FORCING

Results of the two time-dependent, variable forcing simulations show that the circulation patterns of the hourly forcing agree for the most part with those from the daily forcing, except for some transient small-scale phenomena (periods up to several hours). Since the time-dependent simulation is at 1 h time steps, hourly averaging of atmospheric parameters seems most appropriate. Aiming at verifications for mean circulation patterns, we will present only the results of the hourly forcing simulations.

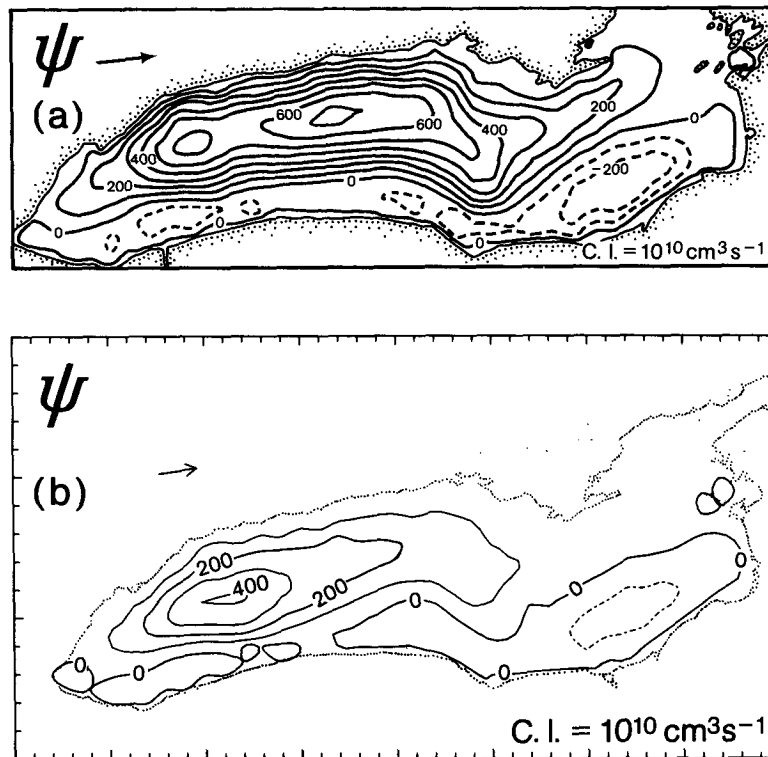


FIG. 2. The simulated transport streamfunction for December 1972 (a) under the monthly mean atmospheric forcing, and (b) under the hourly, spatially varying, time-dependent atmospheric forcing.

Fig. 2b shows the monthly mean transport stream function, and Fig. 4 the monthly mean surface current (Fig. 4a), and currents at corresponding 15 m (Fig. 4b) and 75 m (Fig. 4c) depths as determined by the simulation under the hourly atmospheric forcing. Despite the transient variations and mesoscale eddy phenomena, the monthly mean transport function forms a typical two-gyre circulation pattern from the southwesterly wind, and almost all the eddies are smoothed out. The mean currents are generally flowing eastward, with the mean wind in the shallow regions and return flows, against the mean wind, in the middle of the lake in deep layers. The means of the simulated results of the time-dependent, variable forcing (Figs. 2b and 4) agree nicely with those of the constant forcing (Figs. 2a and 3). The only noticeable differences between Figs. 2a and 2b and between Figs. 3 and 4 are the strengths. The intensity of the streamfunction for the constant forcing is stronger than that of the mean for the time-dependent, variable forcing and so are the currents. This difference might be caused, as we discovered, by the discrepancy between the monthly mean wind speed (Pickett, 1975), which was used to compute the constant-forcing conditions and is the scalar mean of all hourly wind speeds for the month, and the time-dependent wind, which is the observed

hourly vector wind. The former is $\sim 4.5 \text{ m s}^{-1}$, while the monthly mean of the latter is 3.1 m s^{-1} . The differences in strength in transports and velocities of the two states are roughly their wind-stress ratio. Note that in the steady state the current must speed up until balanced by the pressure gradient and the bottom friction, while it is most likely not true in the time-dependent case as pointed out by Simons (1975). The net effect will also result in a stronger circulation pattern in the steady state than in the time-dependent case. It is thus clearly demonstrated that the monthly mean of the hourly time-dependent, variable-forcing simulation does generally merge to the constant-forcing simulation in a homogeneous lake.

b. Summer simulations

Two experiments, one under the monthly mean atmospheric forcing and the other under the hourly, time-dependent and spatially varying atmospheric forcing, were carried out for the July simulation as demonstration cases for summer. The initial conditions for the July simulations were the model results under the monthly mean atmospheric forcing for June 1972 after 30 days integration, starting from the lakewide mean thermal state for 1 June with no

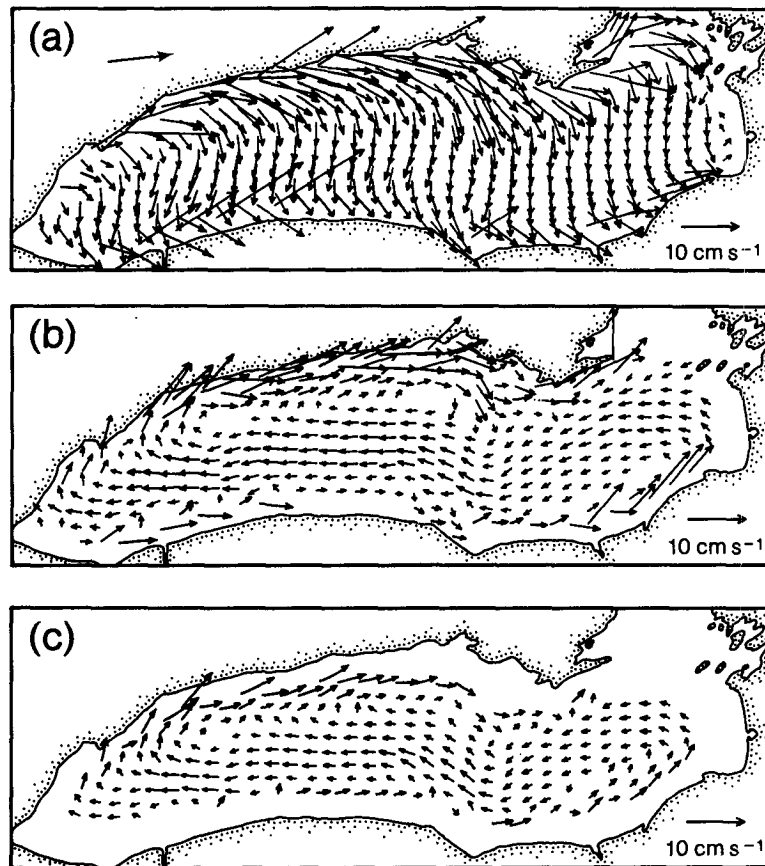


FIG. 3. Simulated December steady-state currents at (a) the surface layer, (b) 15 m depth, and (c) 75 m depth.

motion: the initial condition was the mean state for June. In July 1972 (during IFYGL), except for the last few days of the month, the surface wind was weak (mostly under 1.5 m s^{-1}) and the atmospheric heating was still strong ($\sim 430 \text{ cal cm}^{-2} \text{ day}^{-1}$), with an air temperature 4°C above the water temperature in mid-July (Pickett, 1975).

1) CONSTANT FORCING

The monthly mean July wind is from west-southwest at 3.2 m s^{-1} —similar to the resultant December wind except slightly weaker (Pickett, 1975). Regardless of the difference in density stratification, the steady-state currents of the July simulation also result in a two-gyre wind-driven circulation pattern after a 30-day integration under the monthly mean atmospheric forcing (Fig. 5a), quite similar to that of December. The anticyclonic gyre occupies the northwestern half; the cyclonic gyre stays in the southeastern half of the lake. Magnitudes of the cyclonic and anticyclonic transports are approximately equal. Note that the steady-state anticyclonic gyre in the north is much stronger than the cyclonic gyre in the south of the lake in the December simu-

lation. In the July case, although the wind was similarly uniform and steady, the cyclonic circulation was much stronger than that in December. The relative enhancement of the cyclonic gyre is attributed to the density stratification, as will become clear later in the discussion.

The simulated July currents at the surface and at 15 and 30 m depths are in Fig. 6. Similar to the winter case, the coastal jets are strong, with the wind in the shallow regions, while the surface Ekman currents show in the open lake (Fig. 6a). Returning flows are against the wind in the deeper layers (Figs. 6b and 6c). Note that the simulated currents at the north shore, similar to the result reported by Bennett (1977), are flowing northeastward with the wind, contrasting with the observed mean current in July 1972 (Pickett and Richards, 1975). This also points to the weakness of constant-forcing computations in numerical studies for a stratified lake.

2) TIME-DEPENDENT VARIABLE FORCING

The wind in July 1972 was relatively weak. As a matter of fact, July winds were nearly the weakest during IFYGL except for May winds (Pickett, 1975).

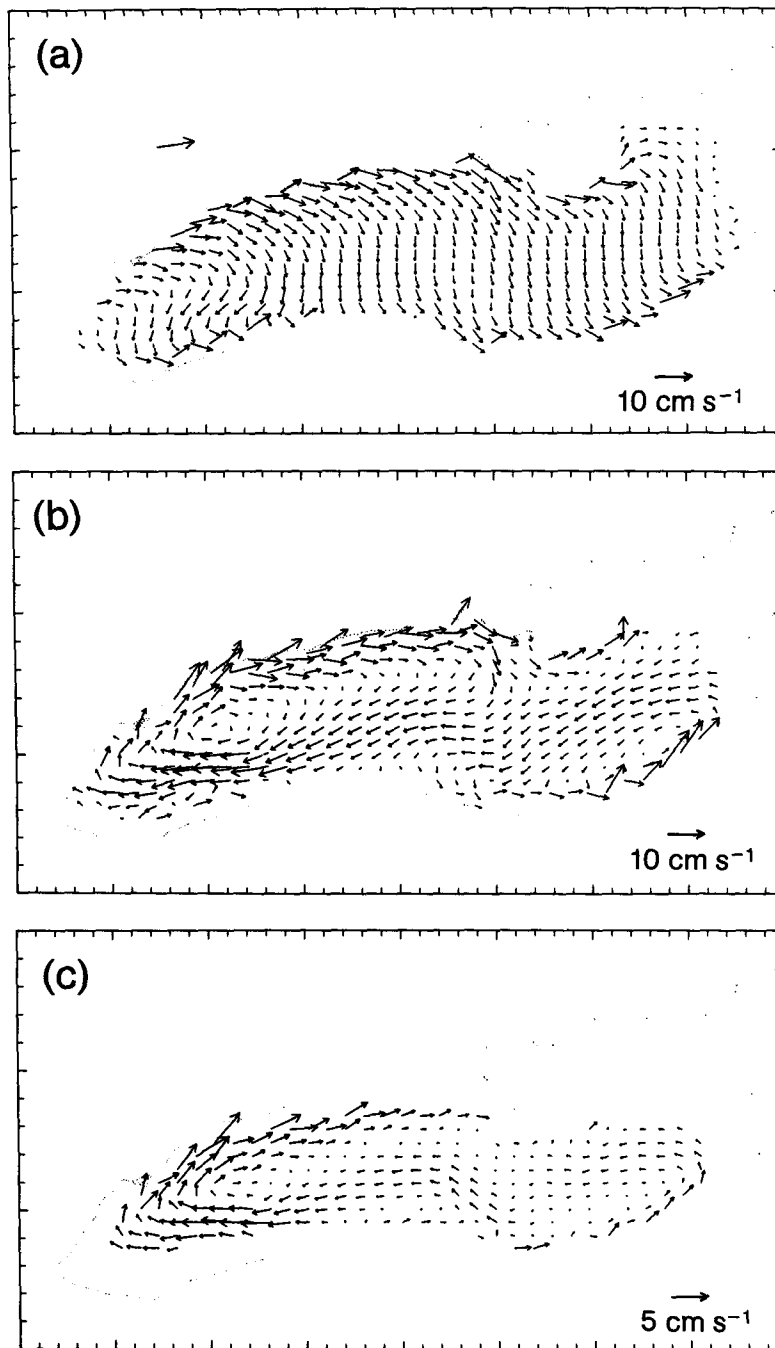


FIG. 4. Monthly mean currents at (a) the surface layer, (b) 15 m depth, and (c) 75 m depth of the hourly time-dependent December simulation.

There was only one wind episode with a relatively short duration (<16 h on the 14th) before the 21st of the month. Before slacking again near the end of the month, there was a strong southwesterly wind of more than 5 m s^{-1} for about 6 days, from the 22nd to the 26th. The hourly simulated currents reveal a persistent cyclonic pattern, with some variation in strength, most of the time before 22 July. Only after

a series of strong westerly episodes from the 22nd to the 26th do the simulated lake currents show several days of the two-gyre wind-driven circulation pattern, a weaker anticyclonic gyre in the northwest and a stronger cyclonic gyre in the southeast. Currents returned to the previous one-gyre, cyclonic pattern again after the wind relaxed on 28 July 1972. The monthly mean of the hourly time-dependent

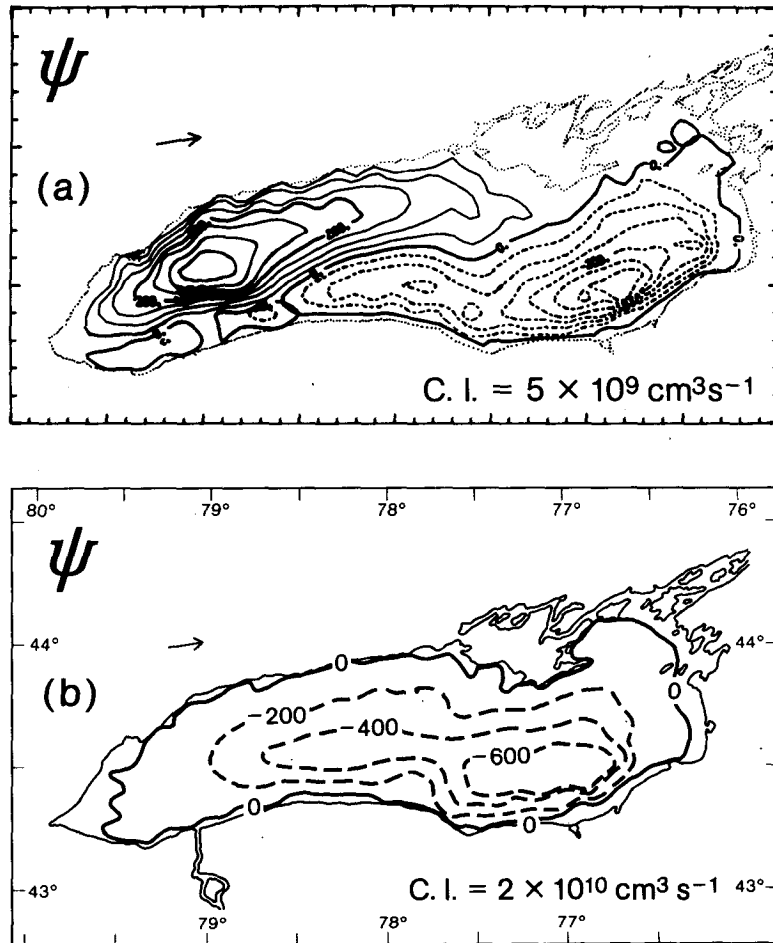


FIG. 5. The simulated transport streamfunction for July 1972 (a) under the monthly mean atmospheric forcing, and (b) under the hourly, spatially varying, time-dependent atmospheric forcing.

transport streamfunction shows a lakewide cyclonic circulation pattern as shown in Fig. 5b. The monthly averages of the time-dependent currents of the layers at the surface and at 15 and 30 m are shown in Fig. 7 for comparison with current meter data. The surface layer circulation pattern (Fig. 7a) reveals a big cyclonic flow, with a strong coastal jet near the south shore and weak currents near the north shore. Individual hourly currents reveal that the surface current at the north shore is sometimes southwestward against the wind when the wind is weak, but it is northeastward with the wind when the wind is relatively strong (over 3 m s^{-1}). Transient currents are generally variable and stronger than the mean current, which is similarly confirmed by observations (Csanady and Scott, 1980). The north shore mean currents are certainly flowing southwestward against the mean wind at the 15 and 30 m depths as observed (Figs. 7b and 7c). Currents at these depths near the north shore are at least as strong as the currents near the south shore. In

general, the time-dependent simulation satisfactorily verifies the observed mean circulation pattern, including the current flowing against the wind near the north shore. July winds during IFYGL were mostly from the west, as the monthly mean wind showed. The Ekman dynamics, then, suggest that flows in the shallow coastal regions will be with the wind, especially along the north shore. Previous studies also show that when the wind is from the west parallel to the longshore axis of the lake, a two-gyre wind-driven circulation pattern prevails. The facts that the prevailing circulation pattern in the time-dependent July simulation is a dominant one-gyre cyclonic pattern and that the mean current in the north shore is flowing against the mean wind indicate that the thermally affected mechanisms are important.

The monthly average temperature of the time-dependent variable-forcing simulation for July 1972 is shown in Fig. 8. Fig. 8a shows that strong horizontal shore-to-shore temperature gradients of $\sim 9^\circ \text{C}$ in the

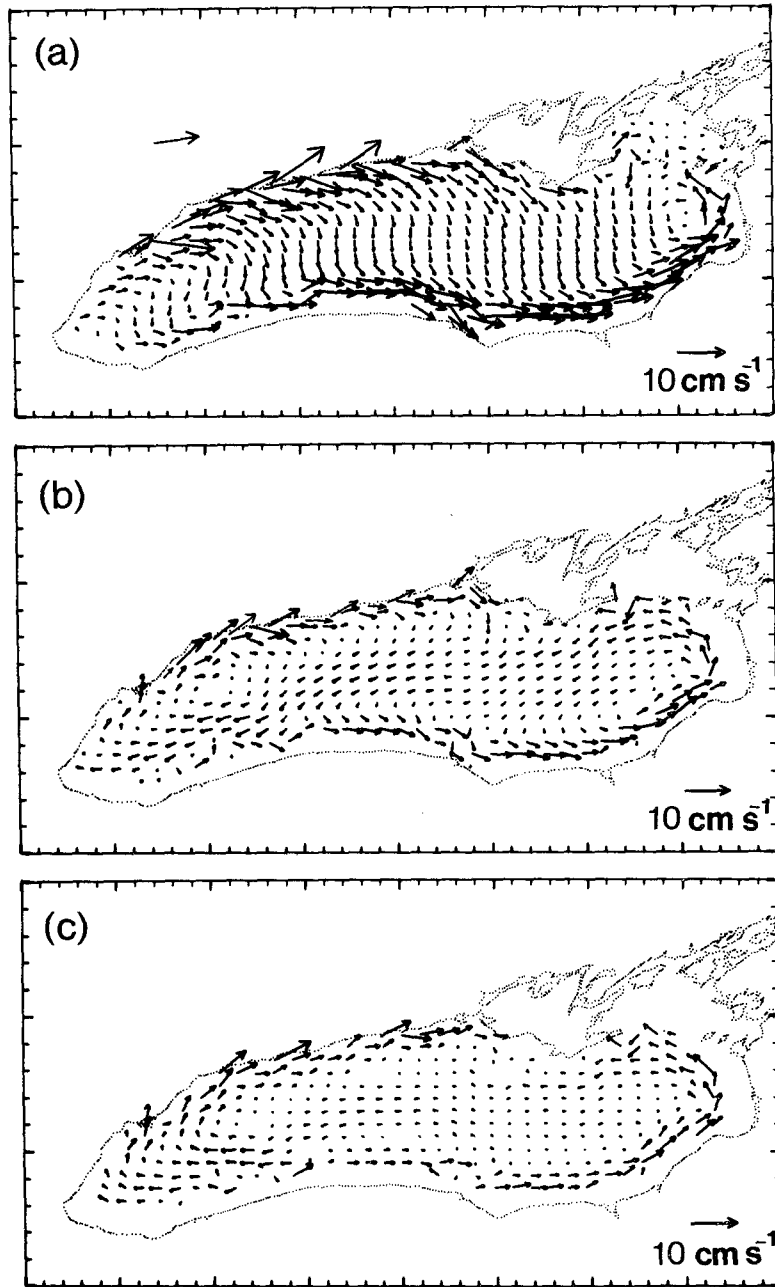


FIG. 6. Simulated July steady-state currents at (a) the surface layer, (b) 15 m depth and (c) 30 m depth.

east-west direction and of $\sim 6^{\circ}\text{C}$ in the north-south direction exist in the surface layer. The same order of magnitude of cross-lake temperature differences exists at the 15 m depth (Fig. 8b); however, the isotherms at 15 m are packed along the southern and the eastern shores, while the northwestern part of the lake is quasi-homogeneous. Similar temperature distributions show in the 30 m depth layer (Fig. 8c). Such a temperature pattern, with decreasing gradients, extends down to more than 100 m. It is ob-

vious from the temperature distribution that the mean shape of isotherm surfaces are concave downward in the lake cross sections because of the accumulations of more warm water along the coastal regions, especially along the perimeter of the central and the eastern portions of the lake (Fig. 8). Such dome-shaped isotherm surfaces will result in a lake-wide mean cyclonic circulation pattern in geostrophic equilibrium with internal pressure fields (Huang, 1971; Csanady, 1977). However, it is not possible

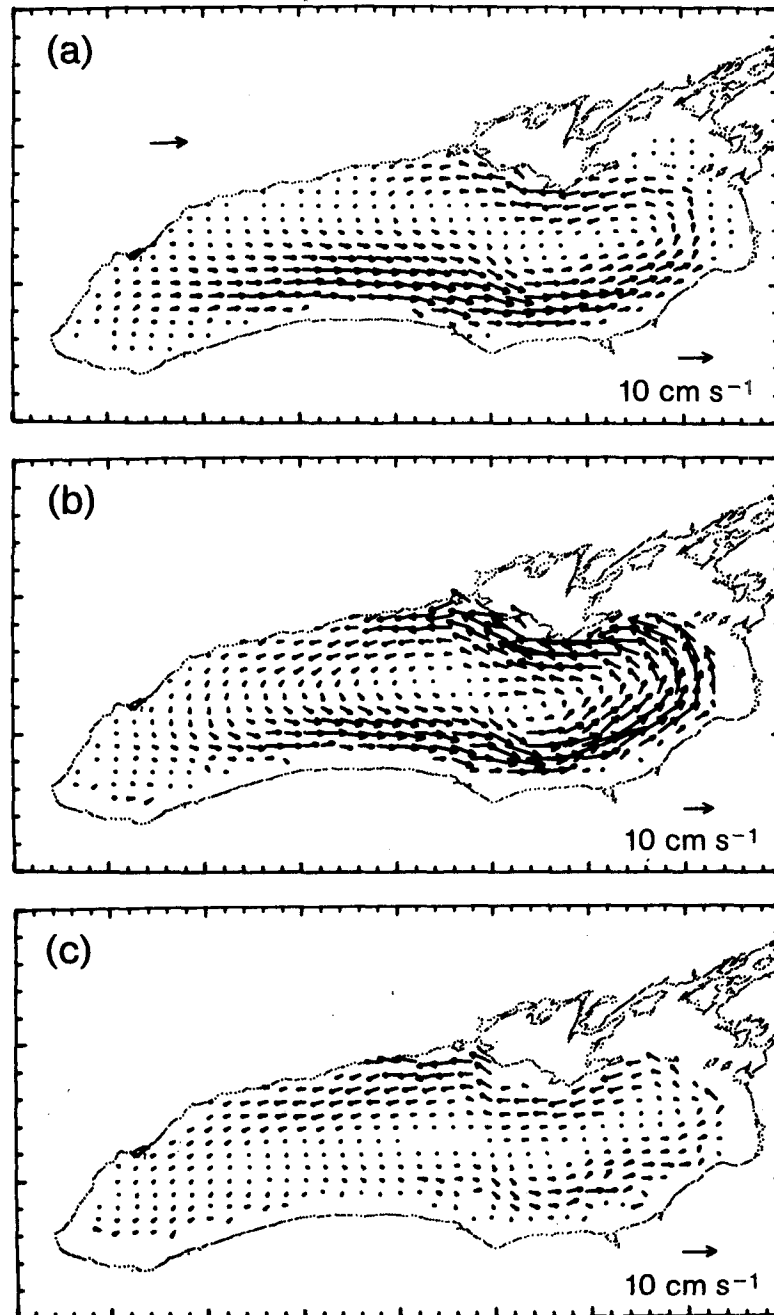


FIG. 7. Monthly mean currents at (a) the surface layer, (b) 15 m depth, and (c) 30 m depth of the hourly time-dependent July simulation.

to analyze the thermocline fluctuations in a more quantitative manner because of the coarse vertical separations of the model.

4. Comparisons and discussion

Since the winter air-water heat flux is from the lake to the atmosphere, the dominant current generating force is the surface wind, which is generally

strong in December. The response of a homogeneous lake is mostly barotropic and swift. Aside from the short-period transient phenomena, the wind-driven currents always result in a counter-rotating two-gyre pattern. The monthly average of the currents from time-dependent variable forcing in December also follows a circulation pattern similar to the one under constant forcing. Aside from transient variations,

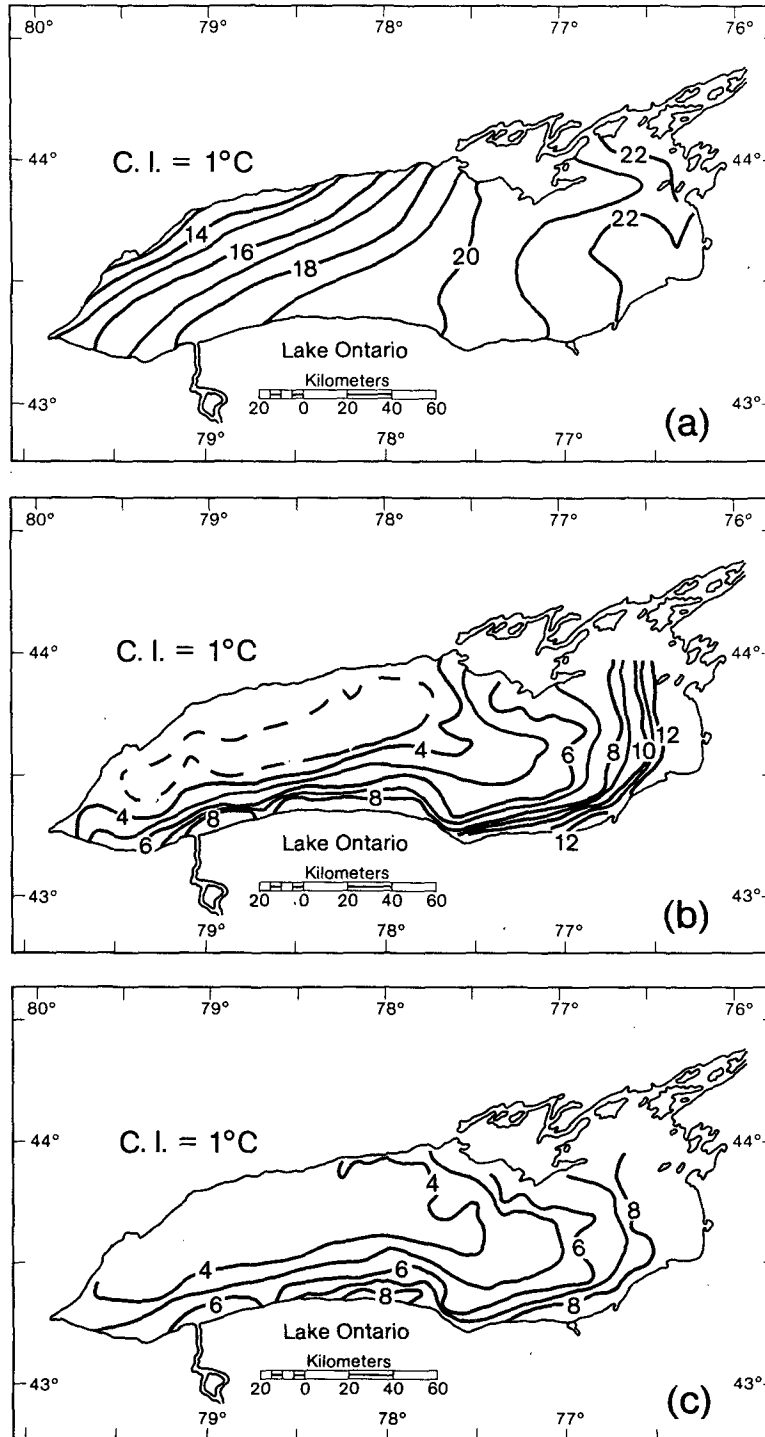


FIG. 8. Monthly mean temperature distributions for (a) the surface layer, (b) the 15 m depth layer (the dotted contour line is 3.5°C), and (c) the 30 m depth layer of the hourly time-dependent July simulation.

there existed two basic patterns in the time-dependent December simulations, a two-gyre circulation pattern with the anticyclonic gyre in the northwest and the cyclonic one in the southeast, or vice versa,

similar to those shown in studies by others (e.g., Csanady, 1975; Rao and Murty, 1970; Simons, 1975; Bennett, 1977). A typical wind-driven double gyre pattern forms after a strong wind, at more than 5

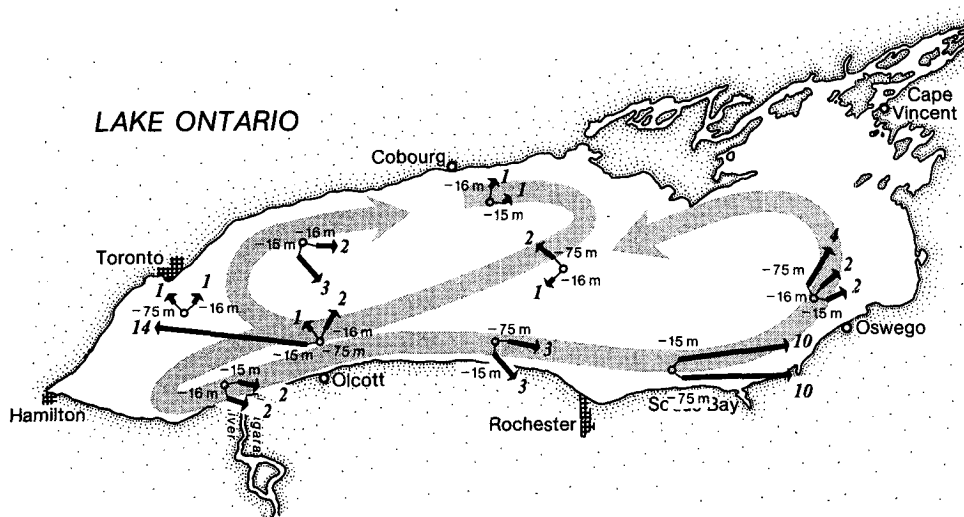


FIG. 9. The observed currents and deduced circulation pattern in Lake Ontario for December 1973 (during IFYGL) (from Pickett, 1977).

m s^{-1} , and blows persistently for several hours; however, as the wind varies in either magnitude or direction, certain transient current patterns in meso-scale eddies, together with large-scale topographic waves, are generated, particularly following strong episodes. Under the equilibrium state of strong wind, the input surface stress in the lake is balanced by the pressure gradient and the bottom friction. The pressure gradient is mostly due to the wind setups at the downwind end, together with some accumulations from the Ekman transports to the right of the wind. As the wind relaxed after the episode, acceleration in the opposite direction developed and mesoscale eddies, together with rotational waves, were generated because of topographic effects and end-boundary reflections, especially in the northeast shallow region near the protruding Pt. Petre, as clearly shown in the time-dependent photographs of circulation patterns (not presented here). The topographic wave propagates cyclonically to the west at a speed of $\sim 60 \text{ cm s}^{-1}$, in fair agreement with Csanady (1976), Simons (1975), and Bennett and Lindstrom (1977). The phenomena of mesoscale eddy generation and the cyclonic propagation of large-scale topographic waves, which can be explained totally by the principle of conservation of potential vorticity, are quite similar to the spindown problem near the eastern boundary of the North Pacific Ocean after the wind system changes (White and McCreary, 1974; McCreary, 1976). Instead of Kelvin waves and Rossby waves, topographic waves are generated in the lake under atmospheric fluctuations (Csanady, 1976).

All current measurements from current meters that survived the severe December weather during IFYGL were processed, and the analyzed observa-

tional results summarized in Fig. 9 (Pickett, 1977). Since no reliable surface current measurements are available, comparisons have been made with respect to the 15 (or 16 m) and the 75 m current patterns. The simulated monthly mean currents at 15 m are shown in Fig. 3b (or similarly in Fig. 4b). We disregard the suspicious westward current of 14 cm s^{-1} at the Olcott station (IFYGL 4), where the normal function of the current meter at 15 m is in doubt after being checked against original data (Pickett, 1980, personal communication). The simulated monthly mean currents then compare very favorably with the monthly mean observed currents. The simulated and the observed current directions at both the 15 and the 75 m level match nearly perfectly, within observational errors, and the only difference between the two is a slight difference in magnitude. Along the southern shore, the agreement in current speeds between the simulation and the observation is generally good. In the middle lake, the verification is excellent; even the direction shift between the 15 and the 75 m level is reproduced. Along the northern shore of the lake the simulated currents at 15 m are slightly stronger than observations. The inferred circulation pattern that fits most observational data is also shown in Fig. 9 (broad gyral arrows). The two-gyre circulation pattern in Fig. 9 coincides acceptably well with the simulated two-gyre pattern of transport function as shown in Fig. 2. Actually, the simulated circulation pattern can fit all the observed currents even better.

Time-dependent station-to-station comparisons between the observations and the simulations reveal only qualitative agreements. As the wind changes, inertial motions are excited. Just as with currents observed in the lake, the simulated currents are con-

taminated with the inertia-period rotary motions, but the effect is even greater in the model. The simulated inertial oscillations are found to be stronger and more prolonged than those observed.

Contrasted to the December case, both the wind-driven and the thermal-driven currents are important in July. Since the variation in temperature is over a relatively long period of time, the mechanisms of producing the thermally driven current are more persistent, and hence in a much longer time scale than those of the wind-driven current. Approaching the end of the lake warm-up season, the horizontal temperature gradients along the perimeter of the eastern half of the lake, as well as meridionally across the lake, remain strong. After the disappearance of the thermal bar feature, shallow thermoclines develop as the season progresses. Thus, the surface water temperature field is greatly influenced by the meteorological factors after stratification. Owing to numerous upwellings and downwellings resulting from the rectified effects caused by wind variations, together with strong surface heating ($\sim 230 \text{ cal cm}^{-2} \text{ day}^{-1}$ in July), a large amount of heat is transported and redistributed in the coastal boundary regions (Fig. 8). The depths of the thermoclines are deeper in the coastal water than in the open lake during the summer stratification. Consequently, the dome shape of the mean isotherm surfaces develops and the lake surface is slightly elevated along the coastal boundary layers and depressed over the center thermocline dome (Csanady, 1977; Bennett, 1978). As a result, there exists a thermally induced cyclonic circulation in addition to the wind-driven pattern in July. Although the surface layer is still under the dominant influence of wind stress, currents in deeper layers are mostly affected by the thermal gradient force. Since the atmospheric scale is much greater than the lake scale, the surface stress input to the lake varies with the water temperature, based on stability arguments as indicated in (2) and (3). The prevailing surface water temperature in July is warmer in the coastal water than in the open lake, warmer along the south shore than along the north, and warmer in the eastern part than in the western region of the lake. As a result of the input surface stress variations due to the changes in drag coefficients affected by the atmospheric stability near the interface, a net vorticity is also generated in the lakewide circulation (Emery and Csanady, 1973). A mean westerly wind, as existed in July 1972, will result in a cyclonic flow in addition to the thermally induced circulation. The persistence of the slowly varying cyclonic circulation results in much less variability in the total lakewide circulation patterns in July. The wind, owing to its great variability, sometimes enhances the cyclonic circulation and more often competes with the thermally induced current. While the wind is weak, although

still from the westerly direction as during most of July, an apparent cyclonic circulation prevails in the time-dependent simulation. Only during the last part of July, from the 22nd to the 26th, does the model lake show a two-gyre circulation pattern with an anticyclonic gyre in the north, after a series of really strong westerly episodes that overwhelmed the thermal influences. It is the thermal effects, which affect the current structure internally and influence the mechanical forcing externally, that compete with the wind-driven current and result in a realistic circulation pattern in a stratified lake.

Published observed July currents for all stations at 15 and 30 m depths, together with dynamic heights during IFYGL, are shown in Fig. 10 (Pickett and Richards, 1975). Overall currents indicate a lakewide cyclonic circulation pattern. Currents along the north shore were flowing westward against the mean wind, while currents along the south shore were with the wind. The monthly mean of the hourly time-dependent circulation pattern for the July simulation is shown in Fig. 5b, and the monthly mean currents for the layers at the surface and at 15 and 30 m are shown in Fig. 7. The time-dependent, average transport streamfunction does merge to form a lakewide cyclonic circulation pattern in good agreement with the overall observed result. The agreements between the simulated currents (Figs. 7b and 7c) and the observed current (Figs. 10a and 10b) are even better. Notice that the simulated and the observed currents along the north shore of the lake are both westward against the mean wind, a result that could not be reproduced from the constant forcing steady-state calculations.

The July mean surface temperature (Chermack, 1977), together with the temperature at 15 and 30 m, as deduced from IFYGL data, are shown in Fig. 11 (Pickett and Richards, 1975). The July mean surface temperature (as shown in Fig. 11a) indicates an average gradient of $\sim 7^\circ\text{C}$ across the lake. The temperature distributions at the 15 and 30 m depths show colder water in the northwestern part of the lake and strong gradients along the south and east shores (Figs. 11b and 11c). The monthly mean temperature of the time-dependent July simulation for the layers at the surface, at 15 and at 30 m are shown in Fig. 8. The model surface temperature generally matches well with the July mean surface temperature, except near the extreme eastern corner. The model produces a similar gradient of from 6 to 7°C across the lake; however, the model temperature in the eastern portion of the lake is $\sim 1^\circ\text{C}$ or more higher than the observational means. Comparison between Fig. 8 and Fig. 11 indicates general agreement in the large-scale features, such as the range and gradient of the surface temperature fields. Comparison of the simulated with the observed temperature fields at 15 and 30 m depths are satisfactory, as shown in Figs. 8b

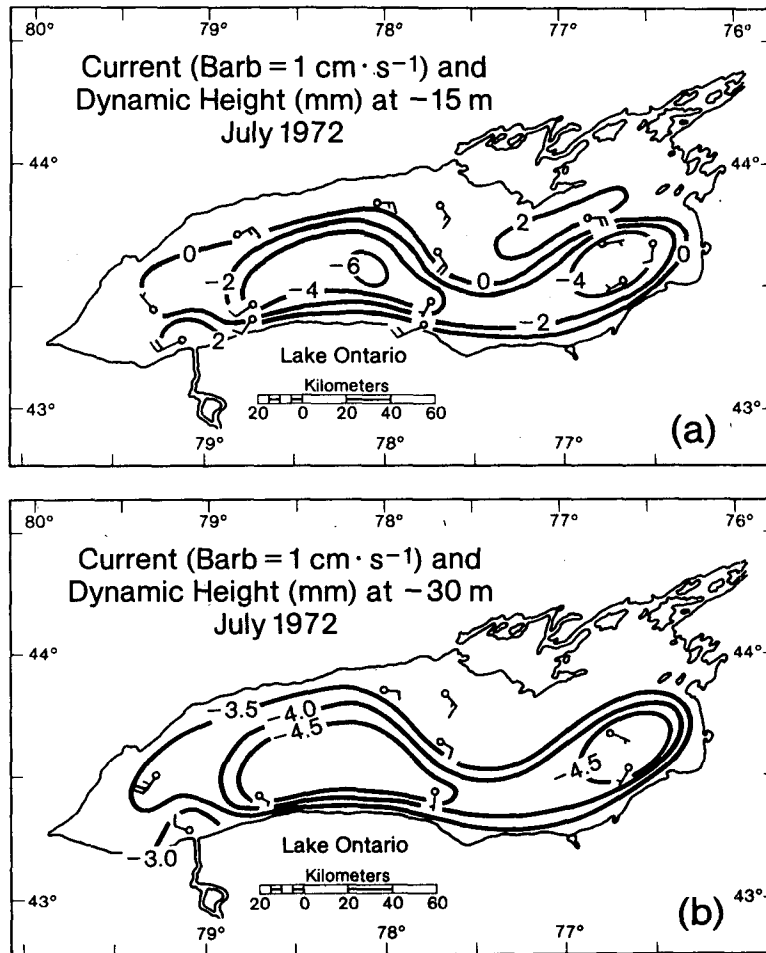


FIG. 10. The observed currents and deduced circulation pattern in Lake Ontario for July 1972 (during IFYGL) (from Pickett and Richards, 1975).

and 8c and Figs. 11b and 11c. The model results, similar to the observations, show a colder water pool near the northwestern part of the lake and stronger gradients along the southeastern shore. However, in the southern and eastern parts of the lake the model temperature is about 3°C cooler at the 15 m depth and 1°C warmer at the 30 m layer than are the IFYGL data. Nevertheless, in both layers the model temperature gradients, which are important to the thermal current generation, are about the same order of magnitude as the observations.

It is obvious from the temperature distribution that isotherms in all cross sections of the lake are dome shaped and generally tilt from southeast to northwest where the water is cooler. It is also obvious that Csanady's mechanism of internal pressure adjustments (1977), resulting from the rectified flows (Bennett, 1978), is actively working toward a mean, geostrophically balanced circulation. As indicated in Fig. 8, the vertical stratification along the south shore is stronger, owing to downwellings, than that along

the north shore, where a quasi-homogeneous state exists because of frequent upwellings. The unevenness in stratification between the north and the south shores may result in a stronger, but shallower, current in the south, as Bennett (1975) suggested, and thus also in a cyclonic circulation. It is even more obvious that the Emery and Csanady (1973) mechanism works in favor of the resultant cyclonic circulation pattern. The surface temperature along the north shore is from about 5 to 6°C lower than that near the south shore (Figs. 8 and 11). According to Deardorff's (1968) formulation, in computing exchange coefficients near the air-water interface with atmospheric stability taken into account, the surface stress along the south shore would be two times as large as that along the north shore, with a horizontal gradient of 6°C or more under the prevailing meteorological conditions. In order to demonstrate this point clearly, we have computed surface stresses for all the IFYGL buoy stations over the lake, based on Eqs. (1), (2), and (3). The results for available

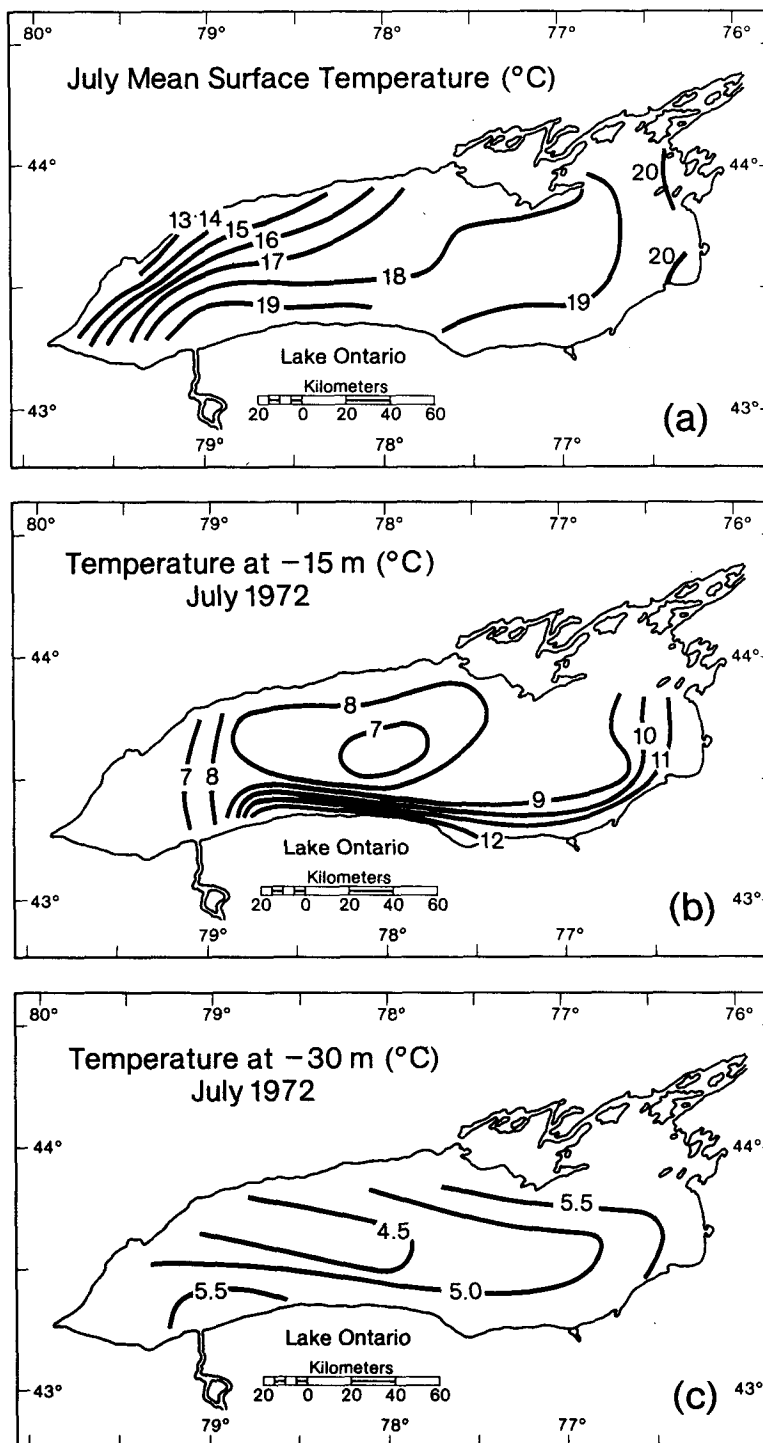


FIG. 11. Mean July temperature at (a) the surface, (from Chermack, 1977) and (b) 15 m depth and (c) 30 m depth in Lake Ontario for July 1972 (during IFYGL) (from Pickett and Richards, 1975).

paired buoy stations whose data were continuous through the whole month of July 1972, and were located in the contrast surface temperature regions in the lake, are summarized in Table 2. Stations 2

and 6 were on the north shore where the surface water was colder in July than was that of stations 4 and 5, their counterparts in the southwestern lake. The surface stresses in the warm region along the

TABLE 2. Mean zonal surface stress (dyn cm^{-2}) and ratio computed from all available paired contrast buoy stations during July IFYGL.

Paired stations	Stress	Paired stations	Stress	Paired stations	Stress
Northshore station (2)	0.14	Northshore station (6)	0.18	West end 3-station mean	0.16
Southshore station (4)	0.27	Southshore station (5)	0.23	East end station (11)	0.37
Ratio	1.96	Ratio	1.26	Ratio	2.31

south shore were from 1.3 to 2 times larger than those along the north shore. For the east to west direction, the east side of the lake is much warmer than the west side, with a temperature contrast of about 7°C in July. The surface stress in the eastern buoy station was two times greater than the mean surface stress for the western stations. Had buoy data in the central region of the lake been available for comparisons, the results would be even more convincing. However, the effectiveness of the Emery and Csanady mechanism has been clearly demonstrated. Even though this surface stress curl may be difficult to observe during fair weather, as indicated in most of the coastal chain data during IFYGL (Csanady and Scott, 1980), air-water temperature differences did prevail intermittently in July 1972, mostly because of the characteristic differences in scales and variabilities between the atmosphere and the lake. It seems that this influential mechanism, together with the other thermally affected mechanisms mentioned above, results in the mean cyclonic circulation in a stratified lake.

5. Summary and conclusions

A numerical dynamic model based on primitive equations, with all major current generating mechanisms taken into account, has been developed for hindcasting the mean state in Lake Ontario during IFYGL. Two simulations, one under the respective monthly mean steady forcing and the other under the respective hourly, time-dependent atmospheric forcing, were carried out in both July and December as representations of summer and winter. An extra run under the daily time-dependent forcing conditions of December reveals only minor deviations in model results (mostly in transient current magnitudes and phases) from those of the hourly forcing. When the lake is homogeneous, in December, Ekman dynamics and wind-driven currents dominate the circulation. The constant-forcing simulation results in a typical two-gyre circulation pattern when the wind blows approximately parallel to the major axis of the lake. In the time-dependent variable-forcing simulation, the high-frequency atmospheric fluctuations have not only excited strong inertial motions, but also generated mesoscale eddies near the downwind end-boundary. Large-scale low-frequency topographic waves, propagating cyclonically at a phase speed of $\sim 60 \text{ cm s}^{-1}$, are also shown in

the simulations. The generation, evolution, and dissipation of topographic waves, as well as mesoscale eddies, can be explained satisfactorily by the principle of conservation of potential vorticity. Despite the noisy inertial oscillations and eddy phenomena, the monthly mean currents of the hourly time-dependent variable-forcing simulation merge to the same two-gyre circulation pattern produced by the December steady forcing.

In the July case, lake dynamics are more complicated owing to the presence of thermal stratifications in addition to the mechanical forcing. With frequent upwellings along the north shore of the lake as the result of the westerly wind episodes, water temperature is colder along the north shore and warmer along the south shore where downwelling occurs. Large-scale vertical movements associated with intermittent upwellings and downwellings redistribute the surface heat transported into the coastal boundary regions by Ekman drifts, as well as the nonlinear rectified effects. As a result, the dome-shaped isotherms develop and strong temperature gradients exist between coastal water and the open lake. Vertical stratification is also stronger in the downwelled coastal water along the south shore than in the upwelled water in the north. The surface stress input along the south shore is also greater, based on atmospheric stability near the surface, than that along the north shore when an average temperature gradient of from 5 to 6°C exists across the lake. All these thermally affected mechanisms, namely, the internal pressure gradient induced by the dome-shaped isotherms, as Csanady (1977) and Bennett (1978) pointed out; the basinwide surface stress curl created by surface temperature differences, as Emery and Csanady (1973) proposed; and the uneven stratifications in the lake, as Bennett (1977) suggested, are working together to result in an apparent cyclonic circulation in a stratified lake. The time-dependent variable-forcing simulation has clearly demonstrated that these important current generating mechanisms are competing with the mechanical forcing in July. The time-dependent transport patterns of the July simulation more frequently reveal the cyclonic, one-gyre circulation pattern that could be forced into the wind-driven two-gyre pattern only after the passage of strong and persistent westerly winds, as shown in the last few days of July 1972. The monthly means of the time-dependent

July currents form a one-gyre cyclonic circulation pattern. The monthly mean currents along the north shore do flow westward against the monthly mean wind, which is westerly. Both the monthly mean currents of the July time-dependent simulation and those of the December simulation match nicely with their respective observed currents and circulation patterns as deduced from IFYGL data. The model temperature distribution also compares well with the observations; hence, the model has been proven capable of reproducing the mean circulation pattern and the general temperature distribution of the observed mean state during IFYGL. It indicates that, for large-scale low-frequency motions in a lake, a relatively coarse-grid model, with ~ 5 km separations, is acceptable, provided the boundary conditions of the atmosphere-lake interactions and the bottom topography are properly treated. Finer mesh-grid separations are proved to strengthen the nonlinear effect, especially in the equatorial and boundary regions (Bennett, 1977; Huang, 1978). However, as far as monthly mean state is concerned, a moderate horizontal separation of ~ 5 km in lake models seems cost effective and adequate. The reason may be that the monthly new circulation patterns in lakes are less affected by the nonlinear transient effects and small-scale features because they were deduced from data smoothed over a time period of a month and collected at monitoring stations that were more widely separated than the model grids.

In contrast to the situation in December, the simulation under the constant monthly mean atmospheric forcing for July does not generate the observed one-gyre circulation pattern produced by the time-dependent, variable-forcing simulation. This is because in December the wind alone dominates current generation in a homogeneous lake, while in July both the wind-driven and the thermal-driven or thermally affected currents are important. Since the response of a large-scale temperature field generally covers a much longer period than does that of the wind, the thermal gradient forcing is more persistent. It is the resultant effect of the total momentum input, which sometimes may possess a stress curl itself, and the total thermal gradient or thermally affected forcing, which generally produces a strong cyclonic vorticity, that determines the apparent current circulation. Under the constant-forcing steady-state simulation in July, the July wind unrealistically overwhelms the thermal forcing. For example, the geostrophically balanced thermal circulation from the dome-shaped isotherms is much weakened owing to the lack of transient variability in upwellings and downwellings in the steady forcing. As expected, the constant-forcing steady-state model produced the typical wind-driven two-gyre circulation pattern with isotherms evenly tilted toward the north in July, which is totally different

from the observational results. This indicates that a constant-forcing steady-state model cannot realistically simulate the mean state in a stratified lake.

Detailed station-to-station comparisons of the time-dependent evolution in lakes reveal that the model responds to wind events faster than do the observations, and that inertial motions are exaggerated in the simulations. The model seems to have underdamped the small-scale, median frequency (inertial) motions and overdamped the large-scale low-frequency motions. The rigid-lid approximation may have some effect on the swiftness of the lake response because there exists no buffer—the free surface oscillations—to temporarily regulate the energy input by transfer to low-frequency (seiche) movements. The characteristics of the discrete layers in the model may also accelerate the dynamic responses. Increased viscosities will reduce the strengths of inertial motions, increased vertical momentum fluxes will suppress the strong shear currents, and decreased bottom friction will improve the magnitude of the long-term mean currents. Some parts of the model temperature distributions in the two near-surface layers generally are from 1 to 3°C higher than observations, indicating there existed stronger or more frequent upwellings near the north shore or an overheating from the atmosphere in the east corner in the model lake. Furthermore, the land-lake breeze (Ching, 1974) and the mesoscale atmospheric high in summer (Lyons, 1971) were not taken into account in the constant forcing calculations. In addition to better atmospheric data, more layers above the thermocline and the use of depth-dependent viscosities and diffusivities (Witten and Thomas, 1976) may improve the thermal structure in the model lake. It appears that an improvement in the partitioning of energy into large-scale low-frequency motions will bring simulations into even closer agreement with IFYGL patterns. More tuning, refinement, and validation of the model are warranted.

Acknowledgments. We wish to express our sincere appreciation to our colleagues, E. J. Aubert, D. B. Rao, R. L. Pickett, J. R. Bennett, and D. J. Schwab, for many helpful discussions and comments. We thank J. R. Bennett in particular for computing the wind stress from IFYGL buoy data with different formulas for comparison, J. Kelley and S. Schneider for editing, and L. Field for typing.

REFERENCES

- Arakawa, A., 1966: Computational design for long-term numerical integration of the equations of fluid motion. Part I. Two-dimensional incompressible flow. *J. Comput. Phys.*, **1**, 119–143.
- Bennett, J. R., 1975: Another explanation of the observed cyclonic circulation of large lakes. *Limnol. Oceanogr.*, **20**, 108–110.
- , 1977: A three-dimensional model of Lake Ontario's sum-

- mer circulation. Part I. Comparisons with observations. *J. Phys. Oceanogr.*, **7**, 591-601.
- , 1978: A three-dimensional model of Lake Ontario's summer circulation. Part II. A diagnostic study. *J. Phys. Oceanogr.*, **8**, 1095-1103.
- , and E. J. Lindstrom, 1977: A simple model of Lake Ontario's coastal layer. *J. Phys. Oceanogr.*, **7**, 620-625.
- Bryan, K., and M. C. Cox, 1967: A numerical investigation of the ocean general circulation. *Tellus*, **19**, 54-80.
- Businger, J. A., J. C. Wyngaard, Y. Izumi and E. G. Bradley, 1971: Flux profile relationships in the atmospheric surface layer. *J. Atmos. Sci.*, **28**, 181-189.
- Chermack, E., 1977: Lake Ontario Atlas: Lake temperatures. N.Y. Sea Grant Inst., NYSSGP-OA-77-008, 41 pp.
- Ching, J. K. S., 1974: A study of lake-land breeze circulation over Lake Ontario from IFYGL buoy observations. *Proc. 17th Conf. Great Lakes Res.*, 259-268.
- Csanady, G. T., 1975: Lateral momentum flux in boundary currents. *J. Phys. Oceanogr.*, **5**, 705-717.
- , 1976: Topographic waves in Lake Ontario. *J. Phys. Oceanogr.*, **6**, 93-103.
- , 1977: On the cyclonic mean circulation of large lakes. *Proc. Nat. Acad. Sci. U.S.*, **74**, 2204-2208.
- , and J. T. Scott, 1980: Mean summer circulation in Lake Ontario within the coastal zone. *J. Geophys. Res.*, **85**, 2792-2812.
- Deardorff, J. W., 1968: Dependence of air-sea transfer coefficients on bulk stability. *J. Geophys. Res.*, **73**, 2549-2557.
- Emery, K. O., and G. T. Csanady, 1973: Surface circulation of lakes or nearly land-locked seas. *Proc. Nat. Acad. Sci. U.S.*, **70**, 93-97.
- Haney, R. L., 1974: A numerical study of the response of an idealized ocean to large-scale surface heat and momentum flux. *J. Phys. Oceanogr.*, **4**, 145-167.
- Huang, J. C. K., 1971: The thermal current in Lake Michigan. *J. Phys. Oceanogr.*, **1**, 105-122.
- , 1972: The thermal bar. *Geophys. Fluid Dyn.*, **3**, 1-25.
- , 1973: A multi-layer regional dynamic model of the North Pacific Ocean. Scripps Inst. Oceanogr. Sci. Ref. No. 73-23, Scripps Institution of Oceanography, La Jolla, Calif.
- , 1977: A general lake circulation model. NOAA Tech. Memo. ERL GLERL-16, 43 pp.
- , 1978: Numerical simulation studies for oceanic anomalies in the North Pacific basin. Part I. The ocean model and the long-term mean state. *J. Phys. Oceanogr.*, **8**, 755-778.
- Lyons, W. A., 1971: Low level divergence and subsidence over the Great Lakes in summer. *Proc. 14th Conf. Great Lakes Res.*, Toronto, Int. Assoc. Great Lakes Research, 467-487.
- McCreary, J., 1976: Eastern tropical ocean responses to changing wind systems with application to El Niño. *J. Phys. Oceanogr.*, **6**, 634-645.
- Pickett, R. L., 1975: Lake-averaged temperatures and currents in Lake Ontario in 1972. *IFYGL Bull.*, **15**, 57-58.
- , 1977: The observed winter circulation of Lake Ontario. *J. Phys. Oceanogr.*, **7**, 153-156.
- , and F. P. Richards, 1975: Lake Ontario mean temperature and currents in July, 1972. *J. Phys. Oceanogr.*, **5**, 755-781.
- Pinsak, A. P., and G. K. Rodgers, 1978: Energy balance panel. *IFYGL Bull.*, **22**, 40-58.
- Rao, D. B., and T. S. Murty, 1970: Calculation of the steady state wind-driven circulations in Lake Ontario. *Arch. Meteor. Geophys. Bioklim.*, **A19**, 195-210.
- Saylor, J. H., J. C. K. Huang and R. O. Reid, 1981: Vortex modes in southern Lake Michigan. *J. Phys. Oceanogr.*, **10**, 1814-1823.
- Simons, T. J., 1974: Verification of numerical models of Lake Ontario. Part I. Circulation in spring and early summer. *J. Phys. Oceanogr.*, **4**, 507-523.
- , 1975: Verification of numerical models of Lake Ontario. Part II: Stratified circulations and temperature changes. *J. Phys. Oceanogr.*, **5**, 98-110.
- , 1976: Verification of numerical models of Lake Ontario. Part III: Long-term heat transport. *J. Phys. Oceanogr.*, **6**, 372-378.
- White, W. B., and J. C. McCreary, 1974: Eastern intensification of ocean spin-down with application to El Niño. *J. Phys. Oceanogr.*, **4**, 295-303.
- Witten, A. J., and J. H. Thomas, 1976: Steady wind-driven currents in a large lake with depth-dependent eddy viscosity. *J. Phys. Oceanogr.*, **6**, 85-92.
- Wunsch, C. L., 1973: On the mean drift in large lakes. *Limnol. Oceanogr.*, **18**, 793-795.